



DOI: 10.11817/j.issn.1672-7347.2022.220086

Trimethylamine oxide induces pyroptosis of vascular endothelial cells through ALDH2/ROS/NLRP3/GSDMD pathway

LI Jialing¹, LÜ Hongwei², CHEN Shuhua³, XIANG Hong², LIU Hengdao⁴, ZHAO Shaoli⁵

1. Department of Cardiology, Third Xiangya Hospital, Central South University, Changsha 410013;
2. Center for Experimental Medicine, Third Xiangya Hospital, Central South University, Changsha 410013;
3. Department of Biochemistry, School of Life Sciences, Central South University, Changsha 410013;
4. Department of Cardiology, First Affiliated Hospital of Zhengzhou University, Zhengzhou 450000;
5. Department of Endocrinology, Third Xiangya Hospital, Central South University, Changsha 410013, China)

ABSTRACT

Objective: Trimethylamine oxide (TMAO) is a metabolite of intestinal flora and is known to promote the progression of atherosclerotic plaques. However, how TMAO works, including its effect on vascular endothelial cells, is not fully understood. This study aims to explore the biological role of TMAO in human umbilical vein endothelial cells (HUVECs) and the underlying mechanism.

Methods: Cell pyroptosis and the loss of plasma membrane integrity were induced under TMAO stimulation in HUVECs. The plasma membrane integrity of the cells was measured by Hoechst 33342/propidium iodide (PI) staining and lactate dehydrogenase leakage assay, and the changes in cell morphology were observed by atomic force microscope. The expression of proteins related to pyroptosis was determined by Western blotting or immunofluorescence. Mitochondrial acetaldehyde dehydrogenase 2 (ALDH2) activity in HUVECs was measured by the ALDH2 activity assay kit, and the level of reactive oxygen species (ROS) was detected by fluorescent probe DCFH-DA.

Results: TMAO induced pyroptotic cell death, manifesting by the presence of propidium iodide-positive cells, the leakage of lactate dehydrogenase, the production of N-terminal gasdermin D (GSDMD-N), and the formation of plasma membrane pores. Moreover, TMAO induced elevated expression of inflammasome components, nucleotide-binding oligomerization domain-like receptor family pyrin domain containing 3 (NLRP3),

Date of reception: 2022-02-18

First author: LI Jialing, Email: 846148171@qq.com, ORCID: 0000-0001-7454-2433

Corresponding author: ZHAO Shaoli, Email: zslplp@163.com, ORCID: 0000-0001-6259-4295

Foundation item: This work was supported by the National Natural Science Foundation (81870352, 81970252, 82000454), the Key Research and Development Project of Hunan Province (2019SK2041, 2020SK2087), and the Joint Project of Medical Science and Technology Research of Henan Province (LHGJ20190092), China.

apoptosis-associated speck-like protein containing a caspase activation and recruitment domain (ASC), and caspase-1 in cells. TMAO significantly inhibited ALDH2 activity and increased intracellular ROS production. However, the activation of ALDH2 by pharmacological manipulation attenuated TMAO-induced inflammasome activation and GSDMD-N production.

Conclusion: TMAO induces pyroptosis of vascular endothelial cells through the ALDH2/ROS/NLRP3/GSDMD signaling pathway, which may be a potential therapeutic target for improving the treatment of atherosclerosis.

KEY WORDS trimethylamine oxide; endothelial cell pyroptosis; endothelial dysfunction; atherosclerosis

氧化三甲胺通过 ALDH2/ROS/NLRP3/GSDMD 通路诱导 血管内皮细胞焦亡

李佳玲¹, 阎宏伟², 陈淑华³, 向红², 刘恒道⁴, 赵少俐⁵

(1. 中南大学湘雅三医院心内科, 长沙 410013; 2. 中南大学湘雅三医院医学实验中心, 长沙 410013;
3. 中南大学生命科学学院生化教研室, 长沙 410013; 4. 郑州大学附属第一医院心内科, 郑州 450000;
5. 中南大学湘雅三医院内分泌科, 长沙 410013)

[摘要] 目的: 氧化三甲胺(trimethylamine oxide, TMAO)是肠道菌群的代谢产物, 可促进动脉粥样硬化斑块的发展。然而, TMAO对血管内皮细胞的作用尚不清楚。本研究旨在探讨TMAO对人脐静脉内皮细胞的生物学作用及其机制。**方法:** 以TMAO刺激人脐静脉内皮细胞诱导细胞焦亡和质膜完整性丧失。采用Hoechst 33342/PI染色法和乳酸脱氢酶释放实验测定细胞质膜完整性, 原子力显微镜观察细胞形态变化。通过蛋白质印迹法或免疫荧光法测定细胞焦亡相关蛋白质的表达。用乙醛脱氢酶2(acetaldehyde dehydrogenase 2, ALDH2)活性测定试剂盒测定人脐静脉内皮细胞中ALDH2的活性, 用荧光探针DCFH-DA检测活性氧(reactive oxygen species, ROS)水平。**结果:** TMAO可诱导内皮细胞焦亡, 表现为细胞死亡增加、乳酸脱氢酶外渗、成孔蛋白GSDMD-N段产生和质膜孔形成。同时, TMAO诱导细胞中炎性体成分核苷酸结合寡聚化结构域样受体蛋白3(nucleotide-binding oligomerization domain-like receptor family pyrin domain containing 3, NLRP3)、凋亡相关微粒蛋白(apoptosis-associated speck-like protein containing a caspase activation and recruitment domain, ASC)和半胱氨酸蛋白酶-1(caspase-1)蛋白质的表达升高。此外, TMAO显著抑制线粒体ALDH2活性并增加细胞内ROS的产生, ALDH2的激活还可减弱TMAO诱导的炎症小体活化和GSDMD-N生成。**结论:** TMAO通过ALDH2/ROS/NLRP3/GSDMD信号通路诱导血管内皮细胞焦亡, 这可能是治疗动脉粥样硬化的潜在靶点。

[关键词] 氧化三甲胺; 内皮细胞焦亡; 内皮功能障碍; 动脉粥样硬化

Blood vessels transport blood to any part of the body, distribute oxygen and nutrients, and remove waste metabolites. Any condition that affects blood circulation can cause vascular disease, usually involving multiple systems. Atherosclerosis is a typical vascular disease that affects arteries. According to data from the 2017 Global Burden of Disease Study, approximately 17.8 million people died of cardiovascular disease worldwide, which has become the primary threat to

human health^[1].

In the pathology of atherosclerosis, endothelial cells are important participants. Vascular endothelial cells form a permeable monolayer along the vascular network for the exchange of substances between circulating blood and tissues. Normally, endothelial cells synthesize and secrete various cytokines to maintain the balance between vasodilation and contraction, inhibition and stimulation of smooth muscle cell proliferation and

migration, thrombosis, and fibrinolysis^[2]. However, once stimulated by certain pathophysiological factors, such as oxidatively modified lipoproteins, advanced glycation end products, reactive oxygen species (ROS), pro-inflammatory cytokines, and hemodynamic disorders^[3], the above-mentioned balances will be broken, and vascular endothelial cells will subsequently undergo various non-adaptive functional changes, including pyroptotic cell death^[4-6].

Different from other forms of cell death such as apoptosis and necrosis, pyroptosis is a pro-inflammatory form of programmed cell death, involving several caspases, mainly caspase-1, -4, -5, and -11^[7]. Nucleotide-binding oligomerization domain-like receptor family, pyrin domain containing 3 (NLRP3)/gasdermin D (GSDMD) pathway is currently considered to be a classic pyroptosis pathway. NLRP3 inflammasomes activated by ROS and metabolic changes drive the cleavage and activation of caspase-1, which in turn cleaves cytosolic GSDMD, leading to the release of N-terminal GSDMD (GSDMD-N) domain. Caspase-4 and -5 in humans and caspase-11 in mice cleave GSDMD through non-canonical inflammasome pathways. The free GSDMD-N, also known as the pore-forming domain, interacts with the plasma membrane, and about 16 domain monomers are oligomerized to form a gasdermin pore^[8]. This pore is required for the secretion of inflammatory interleukin (IL)-1 β and IL-18 into the extracellular space, but it also disrupts the electrochemical concentration gradient across the cell membrane, causing plasma membrane rupture, cell swelling, and cell lysis^[9-12].

Trimethylamine oxide (TMAO) is a biologically active molecule. Its precursor trimethylamine is produced by commensal intestinal bacteria, absorbed in the portal circulation, and then oxidized by heparin-dependent monooxygenase to TMAO^[13]. In vivo, TMAO is important for the normal volume of cells by maintaining the balance of water and electrolytes inside and outside the cell^[14]. TMAO is also a molecular chaperone that stabilizes the folding state of proteins and counteracts the effects of denaturants^[15]. In recent years, many evidences^[16-18] showed that the circulating concentration of TMAO is positively related to the risk of atherosclerosis. Several studies^[19-20] have provided evidence that TMAO may induce endothelial cell

pyroptosis through GSDMD pathway and caspase-3/GSDME pathway, respectively. However, the role of TMAO in endothelial cell pyroptosis and its underlying mechanism remained inadequately investigated.

Mitochondrial acetaldehyde dehydrogenase 2 (ALDH2) is a nuclear-encoded aldehyde oxidase located in the mitochondrial matrix, which detoxifies acetaldehyde endogenously generated aldehydes during lipid peroxidation to protect cells. Recent studies^[21-22] have confirmed that ALDH2 activity is negatively correlated with the severity of atherosclerosis in patients and mice. ALDH2 can reduce the production of mitochondrial ROS (mtROS) and total cellular ROS, inhibit the activation of NLRP3 inflammasomes, prevent cardiomyocyte pyroptosis induced by high glucose, and improve the viability of cardiomyocytes under hyperglycemia^[23]. Conversely, the inhibition of ALDH2 enhances the aging phenotype of vascular endothelial cells, thereby accelerating vascular dysfunction^[24]. So far, the role of ALDH2 in endothelial cell pyroptosis has not been reported.

Therefore, in the study, we speculated that TMAO intervention would induce NLRP3 inflammasome activation and pyroptosis in vascular endothelial cells in vitro and then explored the role of TMAO in human umbilical vein endothelial cells (HUVECs) pyroptosis and the associated mechanisms.

1 Materials and methods

1.1 Reagents

TMAO and ALDH2 activator alda-1 were purchased from Sigma-Aldrich (St. Louis, MO, USA). Primary antibodies against NLRP3 (ab214185), caspase-1 (ab62698), IL-1 β (ab9722), IL-18 (ab191152), GSDMD-N (ab215203) and ALDH2 activity assay kit were purchased from Abcam (Cambridge, MA, USA). Primary antibody against apoptosis-associated speck-like protein containing a caspase activation and recruitment domain (ASC) (sc-514414) was purchased from Santa Cruz Biotechnology (Dallas, TX, USA). BCA protein assay kit, ROS assay kit, and LDH cytotoxicity assay kit were all purchased from Beyotime (Jiangsu, China). Hoechst 33342/propidium iodide (PI) double stain kit was purchased from Solarbio (Beijing, China).

1.2 Cell culture

HUVECs were obtained from American Type Culture Collection grown in endothelial cell medium supplemented with 5% fetal bovine serum, 1% endothelial cell growth factor, and 1% penicillin/streptomycin solution. The cells were incubated at 37 °C in a humidified 5% CO₂ incubator.

Generally, around 80% confluent cells were treated with different concentrations (0, 300, 600, and/or 900 μmol/L) of TMAO for 24 h before further analysis. In different set of experiments, cells were pretreated with alda-1 and then exposed to TMAO for 24 h.

1.3 Hoechst 33342/PI double staining

Hoechst 33342/PI double staining was used to measure plasma membrane integrity and cell death. After washing with phosphate buffered saline (PBS), cells were stained with 2.5 μL Hoechst 33342 staining solution and 2.5 μL PI staining solution in 800 μL cell staining buffer at 4 °C in the dark for 30 min. Cell images were captured with Olympus fluorescence microscope.

1.4 Lactate dehydrogenase leakage assay

The appearance of lactate dehydrogenase (LDH) activity in culture medium as a marker of pyroptotic cell death was measured using a LDH cytotoxicity assay kit. Briefly, 120 μL of cell culture medium and 60 μL of reaction mixture were mixed in a 96-well plate and incubated at room temperature in the dark for 30 min. The absorbance was measured at 490 nm using a PerkinElmer microplate reader. The activity of LDH = (absorbance of test sample/absorbance of control sample maximum enzyme activity) × 100%.

1.5 Atomic force microscopy (AFM)

Cells were seeded in 35-mm Petri dishes. After the treatment, the cells were washed twice with PBS, fixed with 4% paraformaldehyde, and imaged under a force-distance curve-based AFM (FD-based AFM). A Dimension Icon AFM was performed in the PeakForce Tapping mode. The AFM was equipped with a 90 μm piezoelectric scanner. The AFM cantilevers had a nominal spring constant of 0.4 nm⁻¹ and a sharpened silicon tip with a nominal radius of 2 nm. The FD-based AFM topographs were recorded at room temperature (20–24 °C). The AFM was operated within an acoustic

isolation chamber and the maximum force applied to image the samples was 1 nN. The oscillation frequency and oscillation amplitude of the cantilever were set to 2 kHz and 50 nm, respectively. Collected images were analyzed and processed with the Nanoscope Analysis 1.5. Each tapping mode image was flattened to measure the diameter and depth of cell membrane pores. Pore diameters were estimated from both the major axis and short axis around the pore. Pore depths were obtained by measuring from the highest protruding rim relative to the lowest concave edge.

1.6 Western blotting analysis

HUVECs were harvested and suspended in lysing buffer (20 mmol/L Tris-HCl, pH 7.4, 300 mmol/L NaCl, 2% Triton X-100, 2 mmol/L EDTA, and 0.2% SDS) supplemented with protease and phosphatase inhibitors. After agitating for 30 min at 4 °C, cell debris was removed by centrifugation at 15 000 g for 20 min. Protein concentration was determined using a BCA protein assay kit. Extracted proteins were resolved on 10% SDS-PAGE gels and transferred onto polyvinylidene difluoride membranes. The membranes were blocked with 5% non-fat dry milk, washed, and incubated overnight with primary antibodies on a rotary shaker at 4 °C. After washing, the blots were incubated with horseradish peroxidase-conjugated second antibodies for 2.5 h at room temperature, followed by incubation with an enhanced chemiluminescence reagent for 1 min. Protein bands were visualized using an imaging instrument.

1.7 Immunofluorescence assay

Cells were fixed in 4% paraformaldehyde for 15 min and permeabilized by 0.1% Triton X-100 for 15 min. Following blocking at room temperature for 1 h, cells were serially incubated with antibodies against the inflammasome adaptor ASC and IL-1β overnight at 4 °C and fluorescent secondary antibodies for 1 h in the dark. Finally, cells were mounted with 4', 6-diamidino-2-phenylindole (DAPI) and images were captured under Olympus fluorescence microscope.

1.8 Intracellular ROS measurement

Cells were stained with 10 μmol/L fluorescence dye DCFH-DA at 37 °C for 20 min. After washed thrice with serum-free medium, cell images were captured

with Olympus fluorescence microscope.

1.9 Mitochondrial ALDH2 activity assay

Mitochondrial ALDH2 activity in cell lysates was detected using a commercial assay kit according to the manufacturer's instructions. This assay is based on the ability of ALDH2 to catalyse the substrate NAD^+ to produce NADH, which has a strong absorption at 450 nm.

1.10 Statistical analysis

Measurement data were expressed as the mean \pm standard deviation ($\bar{x} \pm s$) and statistically analyzed using SPSS 23.0 software. Independent sample *t*-test was used for the comparison between the 2 groups, and one-way ANOVA was used for the comparison between multiple groups, followed by Dunnett's *t* test for the comparison between the group treated with different concentrations of TMAO and the control group. Other experiments were analyzed using a one-way ANOVA followed by a LSD post hoc test. $P < 0.05$ was considered statistically significant.

2 Results

2.1 TMAO induced the destruction of plasma membrane integrity

To elucidate the relationship between TMAO and vascular endothelial cell pyroptosis, we used HUVECs to evaluate the effect of TMAO on endothelial cell pyroptosis in vitro. After HUVECs were treated with different concentrations (0, 300, 600, 900 $\mu\text{mol/L}$) of TMAO for 24 h and the cell membrane integrity was quantified using Hoechst 33342/PI staining and LDH leakage assay, our results showed that TMAO caused the destruction of the plasma membrane (Figure 1A–1B) and increased the release of LDH (Figure 1C) in a dose-dependent manner.

To characterize the pyroptosis of HUVECs induced by TMAO, we used AFM scanning imaging to observe the perforation of the plasma membrane. Figure 1D shows the formation of pore-like structures of various sizes in the cell membrane 24 h after treatment with 900 $\mu\text{mol/L}$ TMAO. We further used the AFM Nanoscope Analysis software to measure the diameter (horizontal and vertical lengths) and depth of pore-like structures, which confirmed the presence of pores. After TMAO treatment, there were 2 different pores seen in

cell membranes; the pore sizes were 1.5 $\mu\text{m} \times 1.0 \mu\text{m}$ and 1.3 $\mu\text{m} \times 0.6 \mu\text{m}$, and the pore depths were 287 nm and 401 nm, respectively (Figure 1E).

2.2 TMAO increased the expression of pyroptosis-related proteins

In order to understand the molecular mechanism of TMAO-induced pyroptosis of endothelial cells, we evaluated the protein expression levels of NLRP3 inflammasome- and pyroptosis-related components in HUVECs. As shown in Figure 2A–2B, exposure of cells to TMAO led to increased expression of ASC and IL-1 β . Western blotting analysis confirmed that TMAO dose-dependently induced the protein expression of NLRP3, caspase-1, GSDMD-N, and IL-18, and that TMAO had a significant inducing effect on all 4 proteins when it was at 900 $\mu\text{mol/L}$ (Figure 2C – 2D). These results indicated that TMAO-induced pyroptosis of endothelial cells may be at least partially through the canonical inflammasome pathway.

2.3 TMAO inhibited mitochondrial ALDH2 activity and increases total cellular ROS

Determined the changes in ALDH2 activity and ROS production during cell pyroptosis induced by TMAO and found that compared to the untreated control group, 900 $\mu\text{mol/L}$ TMAO significantly reduced ALDH2 activity (Figure 3A), but significantly induced intracellular production of ROS detected by DCFH-DA (Figure 3B). These data indicated that TMAO affects mitochondrial ALDH2 activity and ROS production in vascular endothelial cells.

2.4 ALDH2 activation attenuated ROS accumulation and cell pyroptosis induced by TMAO

As expected, alda-1 pretreatment almost completely abolished the effects of TMAO on ALDH2 activity and ROS production in cells (Figure 4A – 4B). Interestingly, the activation of ALDH2 by alda-1 significantly blunted TMAO-induced increase in expression of NLRP3, caspase-1, and GSDMD cleavage detected by immunoblotting (Figure 4C), suggesting that ALDH2 works upstream of the canonical inflammasome pathway of pyroptosis, and TMAO induces vascular endothelial cell pyroptosis by inhibiting ALDH2 activity (Supplementary Figure 1, <https://doi.org/10.11817/j.issn.1672-7347.2021.220086F1>).

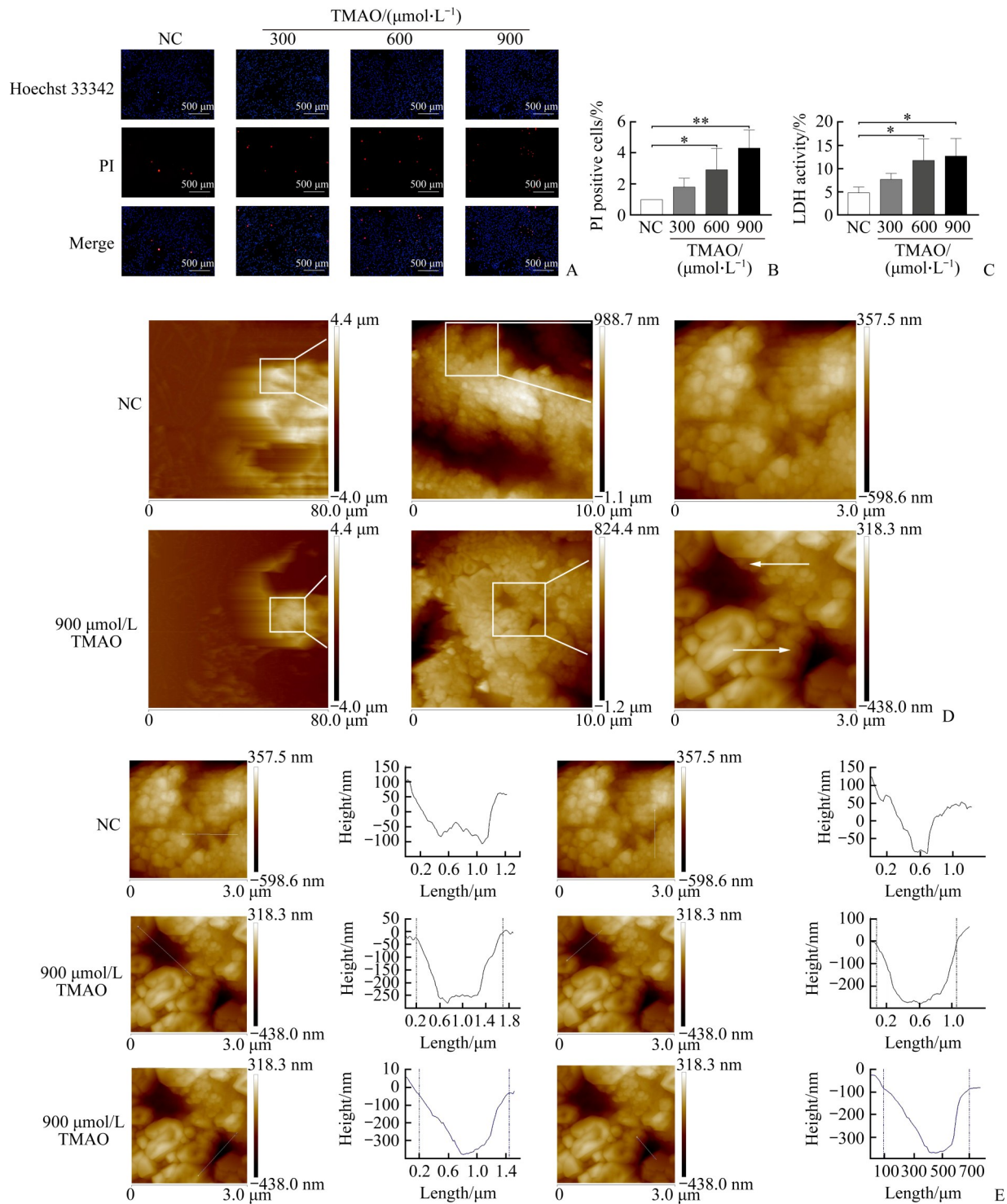


Figure 1 Trimethylamine oxide (TMAO) induces the loss of plasma membrane integrity in human umbilical vein endothelial cells (HUVECs) which are treated with different concentrations of TMAO for 24 h

A: Plasma membrane integrity and cell death were evaluated by Hoechst 33342/propidium iodide (PI) double staining. Low blue/high red (Hoechst 33342+/PI++) represents cell death. B: PI-positive cells were quantitated. C: Lactate dehydrogenase (LDH) released into culture medium as a marker of pyroptotic cell death was measured using a cytotoxicity assay kit. D: Visualization of TMAO-induced pore formation under an atomic force microscopy. E: For diameter measurement, the white lines across the pore served as an indicator of the topography, and the values were calculated between the 2 dotted vertical lines on the curve diagram. Pore depth was defined as the vertical distance between 0 and the lowest value on the curve diagram. Representative images are shown and quantitative data are expressed as the mean \pm standard deviation ($n=3$). * $P<0.05$, ** $P<0.01$.

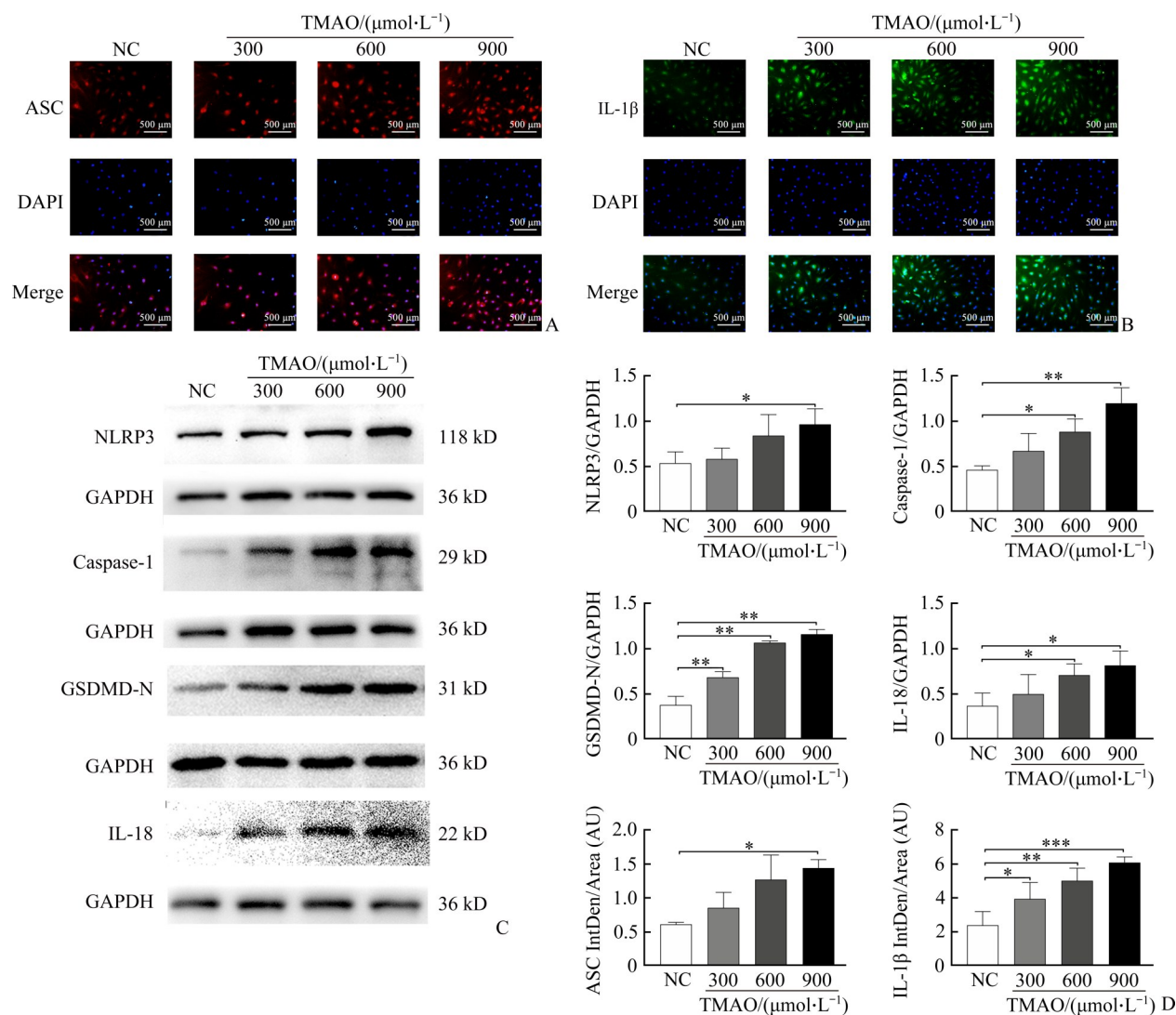


Figure 2 TMAO promotes the expression of inflammasome- and pyroptosis-associated mediators when HUVECs are treated with different concentrations of TMAO for 24 h

A: Inflammasome adaptor apoptosis-associated speck-like protein containing a caspase activation and recruitment domain (ASC) (red) and nucleus (blue) were visualized by immunofluorescence. B: Interleukin (IL)-1 β (green) and nucleus (blue) were detected by immunofluorescence. C: Expression of nucleotide-binding oligomerization domain-like receptor family pyrin domain containing 3 (NLRP3), caspase-1, N-terminal gasdermin D (GSDMD-N), and IL-18 was detected by Western blotting. D: Band densities were quantitated and normalized to the corresponding GAPDH and ASC and IL-1 β intensities were quantitated by immunofluorescence. Representative images are shown and quantitative data are expressed as the mean \pm standard deviation ($n=3$). * $P<0.05$, ** $P<0.01$, and *** $P<0.001$.

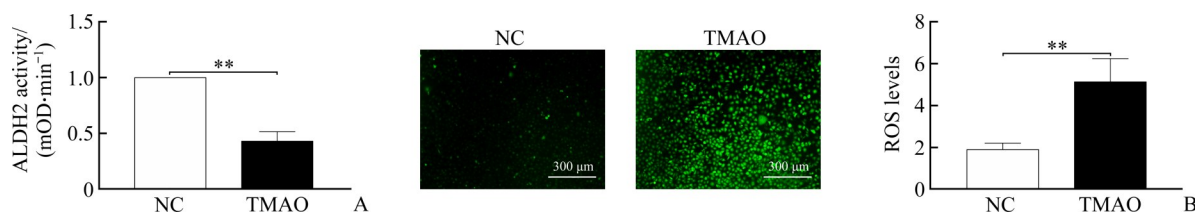


Figure 3 TMAO reduces mitochondrial acetaldehyde dehydrogenase 2 (ALDH2) activity and increases total cellular reactive oxygen species (ROS) when HUVECs are treated with 900 $\mu\text{mol}/\text{L}$ TMAO for 24 h

A: ALDH2 activity was detected by mitochondrial ALDH2 activity assay kit. B: Levels of intracellular ROS were detected by DCFH-DA and quantitated. Representative images are shown and quantitative data are expressed as the mean \pm standard deviation ($n=3$). ** $P<0.01$.

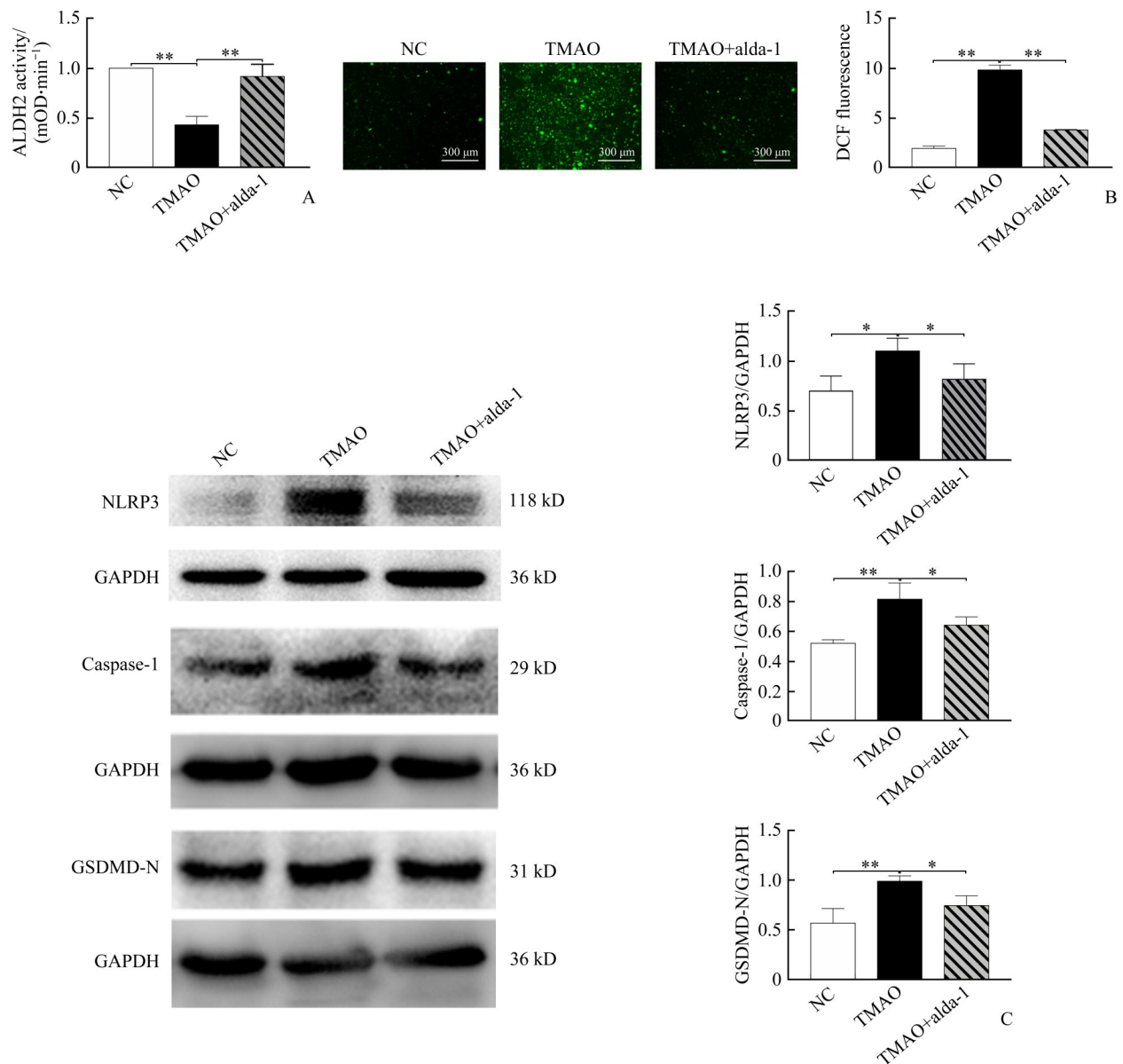


Figure 4 ALDH2 activation attenuates TMAO-induced ROS accumulation and cell pyroptosis when HUVECs are pretreated with ALDH2 activator alda-1 (20 $\mu\text{mol/L}$) for 1 h, and then exposed to 900 $\mu\text{mol/L}$ TMAO for 24 h

A: Mitochondrial ALDH2 activity; B: Intracellular ROS production; C: Expression of NLRP3, caspase-1 and GSDMD-N was detected and quantitated by Western blotting. Representative images are shown and quantitative data are expressed as the mean \pm SD ($n=3$). * $P<0.05$, ** $P<0.01$.

3 Discussion

Currently, accumulated evidence suggests that endothelial dysfunction and pyroptosis contribute to the progression of vascular complications^[25-26]. Also, the role of TMAO in regulating endothelial function is receiving increasing attention^[27-28]. In this study, we collected evidence for the first time that TMAO induces pyroptosis in cultured HUVECs through the ALDH2/

ROS/NLRP3/GSDMD pathway.

Pyroptosis is mainly distinguished from other types of cell death in 3 aspects: Morphological characteristics, immunogenicity, and molecular mechanism. Compared with apoptotic cells, the most significant morphological changes of pyroptotic endothelial cells are the loss of plasma membrane integrity and the release of cell contents. Therefore, we first used Hoechst 33342/PI doubling staining and LDH release assay to assess TMAO-induced cell death. On this basis, in order to

more intuitively characterize the morphological changes of these endothelial cells, we used an AFM to scan the fixed cells. The high-resolution AFM is a tool that uses the force between the probe atoms and the atoms on the sample surface to observe the morphology of the sample, and is widely used in material surface analysis. Recent study^[29] has shown that AFM can accurately capture the plasma membrane pores formed by perforin, complement, and GSDMD-N as well as the high distribution and 3D topographic map of these formed pores, which enables these plasma membrane pores become intuitively visible. For the first time, we measured the pores formed in the plasma membrane of endothelial cells more accurately, and captured high-definition AFM topographic images, which provided direct evidence for vascular endothelial cell death induced by TMAO treatment.

Next, we explored the mechanism of TMAO-associated endothelial cell death. Just like the role of mixed-lineage kinase domainlike in cell membrane perforation in cell necrosis, GSDMD is regarded as the ultimate executor of pyroptosis because of its ability to form pores in the plasma membrane^[30], which eventually leads to cell swelling and osmotic lysis^[31]. We tested the expression level of activated GSDMD-N in endothelial cells treated with different concentrations of TMAO, and found that its expression increased with the increase of TMAO concentration, supporting that endothelial cells undergo pyroptosis following TMAO treatment.

There are several pathways to cause pyroptotic cell death. Inflammatory caspases activated by inflammasome assembly is a key mechanism for the release of GSDMD-N^[32]. We detected the increased expression of inflammatory factors IL-1 β and IL-18 in endothelial cells after TMAO treatment, suggesting that TMAO-induced cell death is accompanied by immune activation. Moreover, increased expression and spikes of ASC in endothelial cells indicate the involvement of inflammasome activation in TMAO cytotoxicity. We also detected the expression level of the inflammasome sensor NLRP3 by Western blotting and demonstrated that NLRP3 expression was up-regulated. These results clearly indicated that TMAO induces HUVEC pyroptosis at least in part through the canonical NLRP3 inflammasome pathway.

Stachowicz, et al^[22] found that ALDH2 has an anti-

atherosclerotic effect in apoE^{-/-} mice. Subsequent studies^[33-35] have confirmed that ALDH2 can reduce oxidative stress, improve mitochondrial dysfunction, and resist cell oxidative damage. In our study, we observed that TMAO induced a decrease in ALDH2 activity and an increase in intracellular ROS levels. Moreover, by using the ALDH2 activator alda-1, we demonstrated that ALDH2 not only controls ROS generation, but also regulates caspase-1 expression and GSDMD-N production. More importantly, ALDH2 is a key negative regulator upstream of TMAO-induced pyroptosis. However, how TMAO reduces ALDH2 activity, such as through direct or indirect action and through enzyme inhibition or genetic manipulation, need to be determined. In addition, TMAO-mediated pyroptosis of vascular endothelial cells and the regulatory role of ALDH2 in the pyroptotic process need to be tested in vivo.

In conclusion, we found that TMAO induces endothelial cell pyroptosis through the ALDH2/ROS/NLRP3/GSDMD pathway, thus revealing the new pathogenesis of TMAO-related vascular dysfunction, which is helpful for designing mechanism-targeted intervention strategies to improve atherosclerotic disease.

Contributions: LI Jialing Research design, experimental operation, and thesis writing; LÜ Hongwei, CHEN Shuhua Research design and thesis revision; XIANG Hong, LIU Hengdao Image analysis and statistical analysis; ZHAO Shaoli Research design, data analysis, dissertation writing and revision. All authors have read and agreed to the final text.

Conflict of interest: The authors declare that they have no conflicts of interest to disclose.

References

- [1] GBD Causes of Death Collaborators. Global, regional, and national age-sex-specific mortality for 282 causes of death in 195 countries and territories, 1980–2017: a systematic analysis for the Global Burden of Disease Study 2017[J]. *Lancet*, 2018, 392(10159): 1736-1788. [https://doi.org/10.1016/S0140-6736\(18\)32203-7](https://doi.org/10.1016/S0140-6736(18)32203-7).
- [2] Medina-Leyte DJ, Zepeda-García O, Domínguez-Pérez M, et al. Endothelial dysfunction, inflammation and coronary artery disease: potential biomarkers and promising therapeutical

- approaches[J]. *Int J Mol Sci*, 2021, 22(8): 3850. <https://doi.org/10.3390/ijms22083850>.
- [3] Gimbrone MA, García-Cardeña G. Endothelial cell dysfunction and the pathobiology of atherosclerosis[J]. *Circ Res*, 2016, 118(4): 620-636. <https://doi.org/10.1161/CIRCRESAHA.115.306301>.
- [4] Xu SW, Ilyas I, Little PJ, et al. Endothelial dysfunction in atherosclerotic cardiovascular diseases and beyond: from mechanism to pharmacotherapies[J]. *Pharmacol Rev*, 2021, 73(3): 924-967. <https://doi.org/10.1124/pharmrev.120.000096>.
- [5] Wang KC, Yeh YT, Nguyen P, et al. Flow-dependent YAP/TAZ activities regulate endothelial phenotypes and atherosclerosis [J]. *Proc Natl Acad Sci USA*, 2016, 113(41): 11525-11530. <https://doi.org/10.1073/pnas.1613121113>.
- [6] Kattoor AJ, Pothineni NVK, Palagiri D, et al. Oxidative stress in atherosclerosis[J]. *Curr Atheroscler Rep*, 2017, 19(11): 42. <https://doi.org/10.1007/s11883-017-0678-6>.
- [7] Man SM, Karki R, Kanneganti TD. Molecular mechanisms and functions of pyroptosis, inflammatory caspases and inflammasomes in infectious diseases[J]. *Immunol Rev*, 2017, 277(1): 61-75. <https://doi.org/10.1111/imr.12534>.
- [8] Ding JJ, Wang K, Liu W, et al. Pore-forming activity and structural autoinhibition of the gasdermin family[J]. *Nature*, 2016, 535(7610): 111-116. <https://doi.org/10.1038/nature18590>.
- [9] Kovacs SB, Miao EA. Gasdermins: effectors of pyroptosis[J]. *Trends Cell Biol*, 2017, 27(9): 673-684.
- [10] Lamkanfi M, Dixit VM. Inflammasomes and their roles in health and disease[J]. *Annu Rev Cell Dev Biol*, 2012, 28: 137-161. <https://doi.org/10.1146/annurev-cellbio-101011-155745>.
- [11] He CL, Zhao Y, Jiang XL, et al. Protective effect of Ketone musk on LPS/ATP-induced pyroptosis in J774A.1 cells through suppressing NLRP3/GSDMD pathway[J]. *Int Immunopharmacol*, 2019, 71: 328-335. <https://doi.org/10.1016/j.intimp.2019.03.054>.
- [12] Shi JJ, Zhao Y, Wang K, et al. Cleavage of GSDMD by inflammatory caspases determines pyroptotic cell death[J]. *Nature*, 2015, 526(7575): 660-665. <https://doi.org/10.1038/nature15514>.
- [13] Zeisel SH, Warrier M. Trimethylamine N-oxide, the microbiome, and heart and kidney disease[J]. *Annu Rev Nutr*, 2017, 37: 157-181. <https://doi.org/10.1146/annurev-nutr-071816-064732>.
- [14] Maiti A, Daschakraborty S. Effect of TMAO on the structure and phase transition of lipid membranes: potential role of TMAO in stabilizing cell membranes under osmotic stress[J]. *J Phys Chem B*, 2021, 125(4): 1167-1180. <https://doi.org/10.1021/acs.jpcc.0c08335>.
- [15] Cho SS, Reddy G, Straub JE, et al. Entropic stabilization of proteins by TMAO[J]. *J Phys Chem B*, 2011, 115(45): 13401-13407. <https://doi.org/10.1021/jp207289b>.
- [16] Zheng LQ, Zheng J, Xie YX, et al. Serum gut microbe-dependent trimethylamine N-oxide improves the prediction of future cardiovascular disease in a community-based general population[J]. *Atherosclerosis*, 2019, 280: 126-131. <https://doi.org/10.1016/j.atherosclerosis.2018.11.010>.
- [17] Tang WHW, Wang ZN, Levison BS, et al. Intestinal microbial metabolism of phosphatidylcholine and cardiovascular risk[J]. *N Engl J Med*, 2013, 368(17): 1575-1584. <https://doi.org/10.1056/NEJMoa1109400>.
- [18] Wang ZN, Roberts AB, Buffa JA, et al. Non-lethal inhibition of gut microbial trimethylamine production for the treatment of atherosclerosis[J]. *Cell*, 2015, 163(7): 1585-1595. <https://doi.org/10.1016/j.cell.2015.11.055>.
- [19] Wu P, Chen JN, Chen JJ, et al. Trimethylamine N-oxide promotes apoE^{-/-} mice atherosclerosis by inducing vascular endothelial cell pyroptosis via the SDHB/ROS pathway[J]. *J Cell Physiol*, 2020, 235(10): 6582-6591. <https://doi.org/10.1002/jcp.29518>.
- [20] Zhou JM, Chen S, Ren J, et al. Association of enhanced circulating trimethylamine N-oxide with vascular endothelial dysfunction in periodontitis patients[J]. *J Periodontol*, 2022, 93(5): 770-779. <https://doi.org/10.1002/JPER.21-0159>.
- [21] Lapenna D, Ciofani G, Ucchino S, et al. Reactive aldehyde-scavenging enzyme activities in atherosclerotic plaques of cigarette smokers and nonsmokers[J]. *Atherosclerosis*, 2015, 238(2): 190-194. <https://doi.org/10.1016/j.atherosclerosis.2014.11.028>.
- [22] Stachowicz A, Olszanecki R, Suski M, et al. Mitochondrial aldehyde dehydrogenase activation by Alda-1 inhibits atherosclerosis and attenuates hepatic steatosis in apolipoprotein E-knockout mice[J/OL]. *J Am Heart Assoc*, 2014, 3(6): e001329[2020-05-14]. <https://doi.org/10.1161/JAHA.114.001329>.
- [23] Cao RP, Fang D, Wang JH, et al. ALDH2 overexpression alleviates high glucose-induced cardiotoxicity by inhibiting NLRP3 inflammasome activation[J]. *J Diabetes Res*, 2019, 2019: 4857921. <https://doi.org/10.1155/2019/4857921>.
- [24] Nannelli G, Terzuoli E, Giorgio V, et al. ALDH2 activity reduces mitochondrial oxygen reserve capacity in endothelial cells and induces senescence properties[J]. *Oxid Med Cell Longev*, 2018, 2018: 9765027. <https://doi.org/10.1155/2018/9765027>.
- [25] Jiang CT, Jiang LP, Li QN, et al. Acrolein induces NLRP3 inflammasome-mediated pyroptosis and suppresses migration via ROS-dependent autophagy in vascular endothelial cells[J]. *Toxicology*, 2018, 410: 26-40. <https://doi.org/10.1016/j.tox.2018.09.002>.
- [26] Gu CF, Draga D, Zhou CD, et al. miR-590-3p inhibits pyroptosis in diabetic retinopathy by targeting NLRP1 and inactivating the NOX4 signaling pathway[J]. *Invest Ophthalmol Vis Sci*, 2019, 60(13): 4215-4223. <https://doi.org/10.1167/iovs.19-27825>.
- [27] Singh GB, Zhang Y, Boini KM, et al. High mobility group box 1 mediates TMAO-induced endothelial dysfunction[J]. *Int J Mol Sci*, 2019, 20(14): 3570. <https://doi.org/10.3390/ijms20143570>.

- [28] Li TJ, Chen YL, Gua CJ, et al. Elevated circulating trimethylamine N-oxide levels contribute to endothelial dysfunction in aged rats through vascular inflammation and oxidative stress[J]. *Front Physiol*, 2017, 8: 350. <https://doi.org/10.3389/fphys.2017.00350>.
- [29] Liu YY, Zhang TZ, Zhou YB, et al. Visualization of perforin/gasdermin/complement-formed pores in real cell membranes using atomic force microscopy[J]. *Cell Mol Immunol*, 2019, 16(6): 611-620. <https://doi.org/10.1038/s41423-018-0165-1>.
- [30] Shi JJ, Gao WQ, Shao F. Pyroptosis: gasdermin-mediated programmed necrotic cell death[J]. *Trends Biochem Sci*, 2017, 42(4): 245-254. <https://doi.org/10.1016/j.tibs.2016.10.004>.
- [31] Jia C, Chen HW, Zhang J, et al. Role of pyroptosis in cardiovascular diseases[J]. *Int Immunopharmacol*, 2019, 67(2): 311-318. <https://doi.org/10.1016/j.intimp.2018.12.028>.
- [32] Xue YS, Enosi Tuipulotu D, Tan WH, et al. Emerging activators and regulators of inflammasomes and pyroptosis[J]. *Trends Immunol*, 2019, 40(11): 1035-1052. <https://doi.org/10.1016/j.it.2019.09.005>.
- [33] Fu SH, Zhang HF, Yang ZB, et al. Alda-1 reduces cerebral ischemia/reperfusion injury in rat through clearance of reactive aldehydes[J]. *Naunyn Schmiedebergs Arch Pharmacol*, 2014, 387(1): 87-94. <https://doi.org/10.1007/s00210-013-0922-8>.
- [34] Gomes KMS, Campos JC, Bechara LRG, et al. Aldehyde dehydrogenase 2 activation in heart failure restores mitochondrial function and improves ventricular function and remodelling[J]. *Cardiovasc Res*, 2014, 103(4): 498-508. <https://doi.org/10.1093/cvr/cvu125>.
- [35] Kang PF, Wang JH, Fang D, et al. Activation of ALDH2 attenuates high glucose induced rat cardiomyocyte fibrosis and necroptosis[J]. *Free Radic Biol Med*, 2020, 146: 198-210. <https://doi.org/10.1016/j.freeradbiomed.2019.10.416>.

(Edited by PENG Minning)

本文引用: 李佳玲, 闫宏伟, 陈淑华, 向红, 刘恒道, 赵少俐. 氧化三甲胺通过 ALDH2/ROS/NLRP3/GSDMD 通路诱导血管内皮细胞焦亡[J]. *中南大学学报(医学版)*, 2022, 47(9): 1171-1181. DOI: 10.11817/j.issn.1672-7347.2022.220086

Cite this article as: LI Jialing, LÜ Hongwei, CHEN Shuhua, XIANG Hong, LIU Hengdao, ZHAO Shaoli. Trimethylamine oxide induces pyroptosis of vascular endothelial cells through ALDH2/ROS/NLRP3/GSDMD pathway[J]. *Journal of Central South University. Medical Science*, 2022, 47(9): 1171-1181. DOI: 10.11817/j.issn.1672-7347.2022.220086